

# Mono- and di-nuclear ruthenium(II) complexes of the ambidentate ligand 3,3'-dihydroxy-2,2'-bipyridine: spectroscopic, electrochemical and mixed-valence properties

Alexander M. W. Cargill Thompson, John C. Jeffery, Davina J. Liard and Michael D. Ward\*

School of Chemistry, University of Bristol, Cantock's Close, Bristol BS8 1TS, UK

The ambidentate, potentially dinucleating ligand 3,3'-dihydroxy-2,2'-bipyridine ( $H_2L$ ) has been shown to co-ordinate to bis(2,2'-bipyridyl)ruthenium(II) fragments in two ways. In  $[Ru(bipy)_2(HL)]X$  ( $X = BPh_4$  **1a** or  $PF_6$  **1b**)  $HL^-$  co-ordinates as a bipy-type  $N,N'$ -chelate; this brings the two hydroxyl substituents of the ligand close together with the result that one of them loses a proton to allow formation of an intramolecular  $O-H \cdots O$  hydrogen bond reminiscent of those found in planar bis(dioxime) complexes. In  $[\{Ru(bipy)_2\}_2(\mu-L)][PF_6]_2$  **2** in contrast the ligand binds in a 'turned-around' mode, acting as an  $N,O$ -chelate to each metal with the two metal centres chemically equivalent. Complex **2** shows two reversible  $Ru^{II}-Ru^{III}$  couples at +0.12 and +0.28 V *vs.* ferrocene-ferrocenium; the separation between these corresponds to a comproportionation constant  $K_c$  of *ca.* 650 for the mixed-valence state, indicative of a class II species, and the electronic spectrum of the  $Ru^{II}-Ru^{III}$  species (generated by chemical oxidation) is also consistent with a valence-trapped (class II) mixed-valence species. Dinuclear complexes in which  $L^{2-}$  acts as an  $N,N'$ -donor to one metal (five-membered chelate ring) and an  $O,O'$ -donor (seven-membered chelate ring) to the other could not be prepared; molecular modelling studies suggest that this binding mode would involve considerable ligand strain.

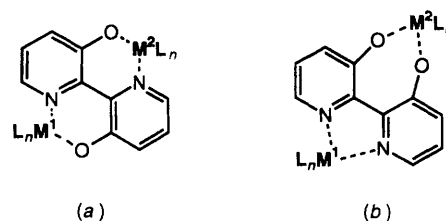
Since the discovery of the Creutz-Taube ion, dinuclear complexes in which the metal fragments are joined by an appropriate bridging ligand have been of particular interest for the study of their mixed-valence properties. Ruthenium-polypyridyl or -amine fragments have been by far the most popular end-groups for studying mixed valency in dinuclear complexes because of their particularly favourable properties: (i) a well established battery of reliable synthetic methods; (ii) reversible metal-centred  $+2/+3$  couples with good kinetic stability in both oxidation states; (iii)  $\pi$ -donor behaviour which ensures strong interactions with  $\pi$ -acceptor bridging ligands and hence strong metal-metal interactions.<sup>1</sup>

In this paper we describe the syntheses, electrochemical and spectroscopic properties of mono- and di-nuclear ruthenium complexes based on the ambidentate bridging ligand 3,3'-dihydroxy-2,2'-bipyridine ( $H_2L$ ). This compound can in principle co-ordinate two metal ions in two different ways (Scheme 1). It could behave symmetrically, presenting an anionic  $N,O$ -binding site to each metal ion, which would result in two six-membered chelate rings; the donor set presented to each metal would be very similar to that of the simple bidentate ligand 2-(2-hydroxyphenyl)pyridine (Hhppy).<sup>2</sup> Alternatively  $H_2L$  could behave asymmetrically, acting as a conventional  $N,N'$ -bipyridyl donor to one metal and a dianionic  $O,O'$ -donor to the other, resulting in one five- and one seven-membered chelate ring. The complexes described herein are the mononuclear complex  $[Ru(bipy)_2(HL)][X]$  ( $X = BPh_4$  **1a** or  $PF_6$  **1b**) and the symmetric dinuclear complex  $[(bipy)_2Ru(\mu-L)Ru(bipy)_2][PF_6]_2$  **2**.

## Experimental

### General details

Proton NMR spectra were recorded on JEOL GX-270 or  $\lambda$ -300 spectrometers, electron-impact (EI) and fast-atom bombardment (FAB) mass spectra (using 3-nitrobenzyl alcohol as matrix) on a VG-Autospec instrument and electronic spectra on Perkin-Elmer  $\lambda$ -2 or  $\lambda$ -19 instruments. Molecular modelling

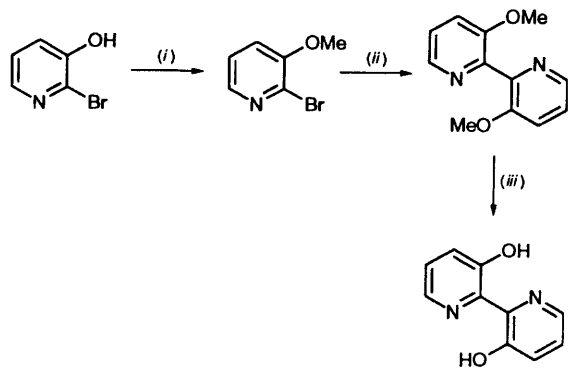


Scheme 1 Symmetric (a) and asymmetric (b) bridging modes of  $L^{2-}$

studies were performed using standard MM2 parameters on a CAChe workstation.

Electrochemical experiments were performed using an EG&G PAR model 273A potentiostat; a standard three-electrode configuration was used, with platinum-bead working and auxiliary electrodes and a saturated calomel electrode (SCE) as reference. Ferrocene was added at the end of each experiment as an internal standard; all potentials are quoted *vs.* the ferrocene-ferrocenium couple. The solvent was acetonitrile, purified by distillation twice from  $CaH_2$ . The base electrolyte was 0.1 mol  $dm^{-3}$   $[NBu_4][PF_6]$ .

Organic starting materials were obtained from Aldrich; ruthenium trichloride hydrate was generously loaned by Johnson Matthey. The complex  $[Ru(bipy)_2Cl_2] \cdot 2H_2O$  was prepared according to the published method.<sup>3</sup> The compound  $H_2L$  was prepared from commercially available 2-bromo-3-hydroxypyridine in three steps (Scheme 2). O-Methylation to give 2-bromo-3-methoxypyridine was carried out exactly according to a published method;<sup>4</sup> homocoupling of this to give 3,3'-dimethoxy-2,2'-bipyridine using a nickel(0) reagent in dmf has also been published,<sup>5</sup> but we found that a more recent modification of this reaction using thf as solvent also worked well and gave a comparable yield.<sup>6</sup> Demethylation of 3,3'-dimethoxy-2,2'-bipyridine to give  $H_2L$  was performed with pyridinium chloride at 190 °C for 2 h.<sup>7</sup> Following neutralisation of the reaction mixture, the luminescent yellow solid was filtered off, washed with water, and dried, giving  $H_2L$  in 93%



**Scheme 2** (i) NaOMe, MeI, dimethylformamide (dmf); (ii)  $[\text{Ni}(\text{PPh}_3)_2\text{Cl}_2]$ , Zn,  $\text{NEt}_4\text{I}$ , tetrahydrofuran (thf); (iii) molten pyridinium chloride

yield. It is clean enough to use for the subsequent complexation reactions; if desired, it may be easily purified by column chromatography on silica with  $\text{CH}_2\text{Cl}_2$  as eluent, and the spectroscopic properties of  $\text{H}_2\text{L}$  obtained by this route are identical to those published earlier.<sup>4</sup>

### Preparations

**Complexes 1a and 1b.** A mixture of  $[\text{Ru}(\text{bipy})_2\text{Cl}_2]\cdot 2\text{H}_2\text{O}$  (0.230 g, 0.44 mmol) and  $\text{H}_2\text{L}$  (0.083 g, 0.44 mmol) in ethylene glycol (10  $\text{cm}^3$ ) was heated with stirring to 160 °C for 1 h. After cooling, addition of aqueous  $\text{NaBPh}_4$  resulted in precipitation of an orange solid which was filtered off and dried. Purification by chromatography on alumina (with MeCN–toluene, 1 : 1 v/v) or flash silica [220–440 mesh, eluting with acetonitrile–water–saturated aqueous  $\text{KNO}_3$  (100:10:1, v/v)], followed by reprecipitation of the complex from the nitrate-containing solutions with  $\text{NaBPh}_4$  afforded pure complex **1a** in ca. 70% yield {Found: C, 70.1; H, 4.7; N, 9.3. Calc. for  $[\text{Ru}(\text{bipy})_2(\text{HL})][\text{BPh}_4]$ : C, 70.5; H, 4.7; N, 9.1%}. FAB mass spectrum:  $m/z$  601  $\{[\text{Ru}(\text{bipy})_2(\text{HL})]^+, 100\%\}$ .

For the purposes of  $^1\text{H}$  NMR spectral characterisation and electrochemical studies, a small amount of complex **1a** was converted into the  $\text{PF}_6^-$  salt **1b** by metathesis in aqueous MeCN with an excess of  $\text{NH}_4\text{PF}_6$ .

**Complex 2.** A mixture of  $[\text{Ru}(\text{bipy})_2\text{Cl}_2]\cdot 2\text{H}_2\text{O}$  (0.425 g, 0.82 mmol) and  $\text{AgNO}_3$  (0.276 g, 2 equivalents) in degassed EtOH–water (1 : 1 v/v, 20  $\text{cm}^3$ ) was heated to reflux for 1 h with stirring under  $\text{N}_2$ . The deep red solution was filtered to remove  $\text{AgCl}$  and then degassed again with a syringe needle. After addition of  $\text{H}_2\text{L}$  (0.077 g, 0.41 mmol) the mixture was heated to reflux for 2 h affording a dark brown solution. After cooling and partial concentration *in vacuo*, addition of aqueous  $\text{NH}_4\text{PF}_6$  resulted in precipitation of a brown solid which was filtered off and dried. Flash chromatography on silica with acetonitrile–water–saturated aqueous  $\text{KNO}_3$  (100:10:1, v/v) resulted in three bands. The orange fraction was mononuclear complex **1** (10–20% yield); the desired symmetric dinuclear complex **2** was the major dark brown fraction and was isolated in 40–55% yield. The fractions containing **2** were concentrated *in vacuo* and precipitated from the remaining water by addition of further  $\text{NH}_4\text{PF}_6$ . After filtration and drying **2** was recrystallised from  $\text{CH}_2\text{Cl}_2$ –hexane to give thin brown plates (Found: C, 48.0; H, 3.9; N, 9.8. Calc. for  $\{[\text{Ru}(\text{bipy})_2\}_2\text{L}\}[\text{PF}_6]_2\cdot \text{C}_6\text{H}_{14}$ : C, 48.4; H, 3.8; N, 10.1%). FAB mass spectrum:  $m/z$  1159 (**2** –  $\text{PF}_6$ , 75) and 1013 (**2** –  $2\text{PF}_6$ , 40%).

## Results and Discussion

### Ligand preparation

The compound  $\text{H}_2\text{L}$  was readily prepared from commercially available 2-bromo-3-hydroxypyridine in three steps (Scheme

2), with some minor variations from the published procedure.<sup>4</sup> The coupling of 2-bromo-3-methoxypyridine using a phosphine nickel(0) catalyst in dmf has been described,<sup>5</sup> but we found that the reaction was more conveniently carried out using the recent modification of Iyoda *et al.*<sup>6</sup> which uses  $\text{NEt}_4\text{I}$  as an additional component of the catalyst and thf as solvent. The yields of the two methods are comparable but the latter route provides an easier work-up due to the ease with which thf may be removed, and a lower degree of contamination of the product with  $\text{Ph}_3\text{PO}$ . Demethylation of the 3,3'-dimethoxy-2,2'-bipyridine to give  $\text{H}_2\text{L}$  has been carried out with  $\text{BBr}_3$  in 60% yield,<sup>4</sup> but we found that pyridinium hydrochloride<sup>7</sup> at 190 °C gave a near-quantitative yield of  $\text{H}_2\text{L}$ . Despite its obvious appeal as a bridging ligand, no co-ordination chemistry of  $\text{H}_2\text{L}$  has yet been reported.

### Synthesis and characterisation of complex 1a

Reaction of  $\text{H}_2\text{L}$  with  $[\text{Ru}(\text{bipy})_2\text{Cl}_2]\cdot 2\text{H}_2\text{O}$  in a 1 : 1 ratio resulted in good yields of the mononuclear complex  $[\text{Ru}(\text{bipy})_2(\text{HL})][\text{X}]$  ( $\text{X} = \text{BPh}_4^-$  **1a** or  $\text{PF}_6^-$  **1b**). That the ligand has retained one proton, affording a monocationic complex cation, is apparent from the FAB mass spectrum and elemental analytical data. The  $^1\text{H}$  NMR spectrum of **1b** (Fig. 1; the hexafluorophosphate salt was used to prevent interference from the phenyl protons of the  $[\text{BPh}_4]^-$  anion of **1a**) shows that the complex has two-fold symmetry, with 11 aromatic proton environments each of relative intensity 2 H; the remaining proton of  $\text{HL}^-$  gives a broad singlet at  $\delta$  18.1 the integral of which corresponds to 1 H. The two-fold symmetry indicates that  $\text{HL}^-$  is symmetrically co-ordinated *via* the two N atoms as a conventional bipy-type donor and not as an N,O-donor. Co-ordination of  $\text{H}_2\text{L}$  to a metal ion in this way will bring the two 3-hydroxy groups into close contact. Whilst this steric interference is not sufficient to prevent co-ordination—other bipy derivatives with substituents at the 3 and 3' positions are known to co-ordinate effectively<sup>8</sup>—it results in loss of one hydroxyl proton such that the remaining proton interacts with both oxygen atoms *via* an intramolecular hydrogen bond, in the manner of  $[\text{Ni}(\text{Hdmg})_2]$  ( $\text{H}_2\text{dmg} = \text{dimethylglyoxime}$ ).<sup>9</sup> A molecular mechanics-based energy-minimised structure of **1** suggested that the two oxygen atoms are 2.45 Å apart. This close contact suggests formation of a strong, symmetrical  $\text{O}\cdots\text{H}\cdots\text{O}$  hydrogen bond,<sup>10</sup> and is very similar to the separation between oxygen atoms in  $[\text{Ni}(\text{Hdmg})_2]$ .<sup>9</sup> The highly electronegative environment of this proton is confirmed by its position of  $\delta$  18.1 in the  $^1\text{H}$  NMR spectrum; in contrast, if  $\text{HL}^-$  were co-ordinated as an N,O-chelate, the remaining proton in the external N,O pocket would resonate at about  $\delta$  15.<sup>2,11</sup>

### Synthesis and characterisation of complex 2

Reaction of  $\text{H}_2\text{L}$  with 2 equivalents of  $[\text{Ru}(\text{bipy})_2\text{Cl}_2]\cdot 2\text{H}_2\text{O}$  in ethanol afforded a reaction mixture which contained (by TLC analysis) substantial amounts of mononuclear complex **1** in addition to a new dark brown material. A more satisfactory method of driving the reaction nearer to completion was to pre-treat the  $[\text{Ru}(\text{bipy})_2\text{Cl}_2]\cdot 2\text{H}_2\text{O}$  with  $\text{AgNO}_3$  in aqueous ethanol, which affords a deep red solution containing the substitution-labile complex  $[\text{Ru}(\text{bipy})_2(\text{H}_2\text{O})_2]^{2+}$ . Reaction of this with 0.5 equivalent  $\text{H}_2\text{L}$  gave a mixture containing much smaller amounts of **1**, and large amounts of a dark brown fraction, complex **2**, which could be isolated in typically ca. 50% yield.

The formulation of complex **2** as  $[(\text{bipy})_2\text{Ru}(\mu\text{-L})\text{Ru}(\text{bipy})_2][\text{PF}_6]_2$  was established from FAB mass spectrometry and elemental analysis. The presence of 19 aromatic proton environments in the  $^1\text{H}$  NMR spectrum (Fig. 2) shows that the complex has two-fold symmetry; the assignments are based on a  $^1\text{H}$ – $^1\text{H}$  correlation (COSY) spectrum. Sixteen proton environments are apparent between  $\delta$  7.0 and 9.2 for the four types of

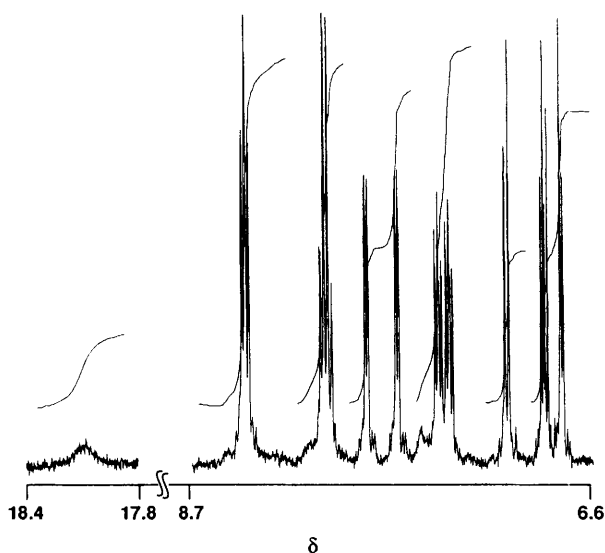


Fig. 1 Proton NMR spectrum of complex **1b** in  $\text{CD}_2\text{Cl}_2$

pyridyl ring; the three proton environments in the bridging ligand occur between  $\delta$  6.0 and 6.2. That the bridging ligand is acting as two N,O-donors to give chemically equivalent metal centres is confirmed by the electrochemical and electronic spectral properties as well as a partial crystal structure (see below).

#### Partial crystal structures of complexes **1a** and **2**

Additional confirmation of the structures of complexes **1** and **2** is provided by partial crystal structures (Figs. 3 and 4).<sup>\*</sup> The quality of these is too poor to warrant any detailed discussion of structural parameters, but the gross structures are clear and confirm the co-ordination modes of the ligands that were evident from spectroscopic data, and the diagrams are included solely on that basis.

#### Electronic spectroscopy of complexes **1**

The electronic spectrum of complex **1a** in  $\text{CH}_2\text{Cl}_2$  (Fig. 5) displays two absorptions at 436 and 481 nm ( $\epsilon = 1.5 \times 10^4$

<sup>\*</sup> Numerous attempts were made to grow X-ray-quality crystals of complexes **1** and **2**, using a variety of different counter ions ( $\text{PF}_6^-$ ,  $\text{BPh}_4^-$ ,  $\text{ClO}_4^-$ ) and solvent combinations. For both complexes only small, poor-quality crystals were obtained which diffracted weakly. For **1a** the crystals (from  $\text{CH}_2\text{Cl}_2$ -hexane) grew as very thin plates, and the best single crystal we could find had a thickness of only 0.03 mm. The only crystals of **2** (also from  $\text{CH}_2\text{Cl}_2$ -hexane) were likewise thin leaves which cracked in seconds when removed from the mother-liquor. The results here are the best of several attempts in each case. The crystals were rapidly transferred from the mother-liquor to a cold  $\text{N}_2$  stream ( $-100^\circ\text{C}$ ) on the diffractometer (a Siemens SMART). Unit-cell data: **1a**, monoclinic, space group  $P2_1/c$ ,  $a = 12.289(4)$ ,  $b = 13.590(6)$ ,  $c = 31.49(2)$  Å,  $\beta = 100.03(3)^\circ$ ,  $U = 5194(4)$  Å<sup>3</sup>;  $Z = 4$ ; **2**, triclinic, space group  $P\bar{1}$ ,  $a = 9.816(9)$ ,  $b = 19.21(2)$ ,  $c = 19.59(2)$  Å,  $\alpha = 100.16(9)$ ,  $\beta = 94.37(9)$ ,  $\gamma = 96.13(8)^\circ$ ,  $U = 3599(7)$  Å<sup>3</sup>. The data sets in both cases did permit solution of the structures, but the levels of refinement are poor [ $R$  for selected data with  $I > 2\sigma(I)$  and  $2\theta_{\text{max}} = 46.5^\circ$  was 0.14 for **1a** and 0.18 for **2**]. This may be ascribed to a combination of the small sizes and poor quality of the crystals, and the rapidity with which they lost solvent. Consequently, the full structural details are not of publishable quality and it is not possible to extract accurate bond lengths and angles. However, the gross structures of the complex cations are quite well defined and confirm the important points that were apparent from the spectroscopic data: *i.e.* for **1a**,  $\text{HL}^-$  is co-ordinated as an N,N-donor, and there is only one  $\text{BPh}_4^-$  anion per complex cation; for **2**,  $\text{L}^{2-}$  is co-ordinated as two N,O-donors with two six-membered chelate rings. This 'turn-around' binding mode of  $\text{L}^{2-}$  in **2** is similar to that observed in the ambidentate ligand 3-amino-6,6'-dimethyl-2,2'-bipyridine, which has a choice of bipyridyl or pyridyl-amine co-ordination modes.<sup>12</sup>

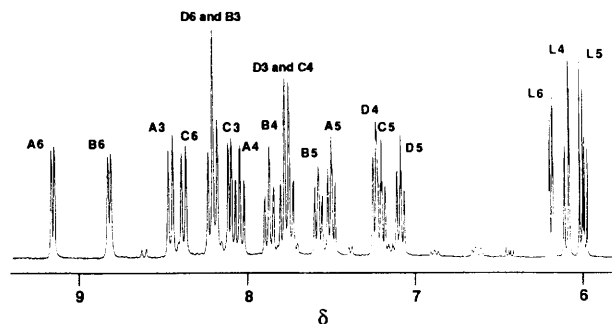


Fig. 2 Proton NMR spectrum of complex **2** in  $\text{CD}_2\text{Cl}_2$ . The labels A–D denote the four independent pyridyl rings; L denotes the bridging ligand. The numerals 3–6 denote the position of the proton on the pyridyl ring

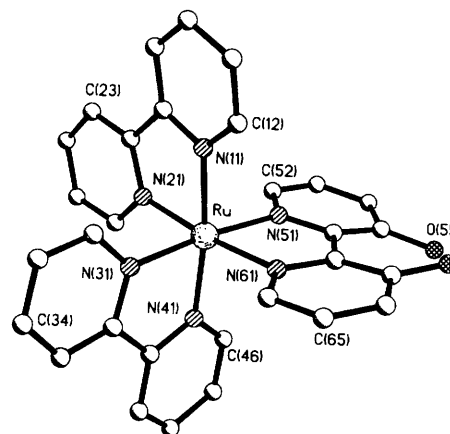


Fig. 3 Structure of the cation of complex **1a** from a partial crystal analysis

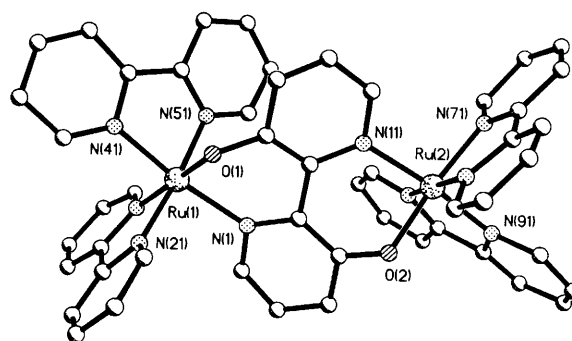


Fig. 4 Structure of the cation of complex **2** from a partial crystal analysis

and  $1.0 \times 10^4 \text{ dm}^3 \text{ mol}^{-1} \text{ cm}^{-1}$  respectively), which are characteristic of metal-to-ligand charge-transfer (m.l.c.t.) transitions for  $[\text{Ru}(\text{bipy})_3]^{2+}$ -type chromophores.<sup>13</sup> There are shoulders on the high-energy side of the main m.l.c.t.-transition which may be higher-energy m.l.c.t. processes, and the usual intense ligand-based  $\pi-\pi^*$  transitions are apparent in the UV region.

The presence of a deprotonated oxygen atom on the periphery of  $[\text{HL}]^-$  in complex **1** should render the ligand more strongly  $\pi$ -basic than an unsubstituted bipyridine, since the negative charge of one oxygen atom can be transferred onto the nitrogen atom of the other ring (Scheme 3).<sup>14</sup> This would have the effect of red-shifting the m.l.c.t. bands of the absorption spectrum, since the metal  $d(\pi)$  orbitals would be raised in energy and brought closer to the ligand  $\pi^*$  orbitals. For example, deprotonation of the two hydroxyl groups of 4,7-dihydroxy-1,10-phenanthroline (dhphe) in complexes of the type  $[\text{Ru}(\text{L-L})_2(\text{dhphe})]^{2+}$  (L-L denotes a bipyridine derivative)

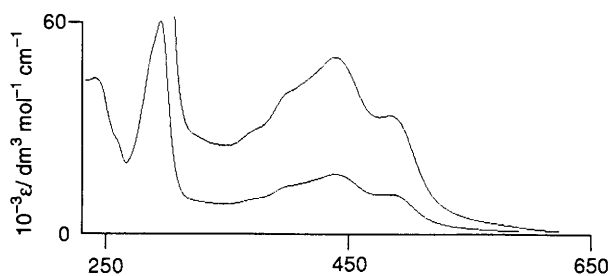
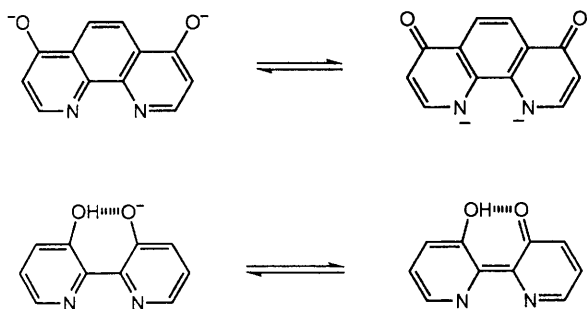


Fig. 5 Electronic spectrum of complex **1a** in  $\text{CH}_2\text{Cl}_2$  (expansion is 3)



Scheme 3 Tautomeric forms of deprotonated 4,7-dihydroxyphenanthroline (top) and  $[\text{HL}]^-$  (bottom)

results in a red shift of the principal m.l.c.t. transition from *ca.* 450 to *ca.* 500 nm.<sup>14</sup> This effect does not seem to operate so strongly in **1**, probably because the presence of the hydrogen-bonded proton in  $[\text{HL}]^-$  stabilises the valence tautomer in which the negative charge is localised on the oxygen atoms rather than transferred to the nitrogen atoms. The equilibrium of Scheme 3 lies to the left more than it would for *dhphen*, and  $\text{HL}^-$  behaves more like a conventional bipy-type ligand.

Ruthenium-polypyridine complexes with pendant pH-sensitive functional groups (such as OH groups, or the peripheral NH group of a co-ordinated benzimidazole) have been of interest because of the possibility of varying their redox and spectroscopic properties by a pH-switching mechanism.<sup>14</sup> In order to examine the pH sensitivity of the  $\text{O}\cdots\text{H}\cdots\text{O}$  hydrogen-bond fragment we examined the electronic spectrum of **1** in water as a function of pH. The complex could be rendered water-soluble by dissolving in MeCN, adding an equal volume of saturated aqueous  $\text{KNO}_3$ , and then removing the MeCN *in vacuo*, thus forming the water-soluble  $[\text{Ru}(\text{bipy})_2(\text{HL})][\text{NO}_3]$ . Spectra of the complex were recorded over the range pH 0.4–13.6 (the limits of usability of the pH electrode), using  $\text{HNO}_3$  or  $\text{NaOH}$  to control the pH (the ionic strength of the solutions was kept effectively constant since they were saturated in  $\text{KNO}_3$ ). Over the range pH 2–13.6 there was no significant change in the position or intensity of any of the spectral bands. At pH values more acidic than 2 a sharp increase in the intensity of the  $\pi \rightarrow \pi^*$  ligand-centred transition at 298 nm occurred: the absorption coefficient rose from  $70\,000\text{ dm}^3\text{ mol}^{-1}\text{ cm}^{-1}$  at pH 2 to *ca.*  $400\,000\text{ dm}^3\text{ mol}^{-1}\text{ cm}^{-1}$  at pH 0.4 (Fig. 6). This intense new transition is presumably associated with the (fully protonated)  $\text{H}_2\text{L}$  ligand, since nothing of that intensity occurs in the spectrum of  $[\text{Ru}(\text{bipy})_3]^{2+}$ .<sup>13</sup> We could not use more acidic solutions because of the limitations of our pH electrode but it appears that the *pK* value for protonation to give  $[\text{Ru}(\text{bipy})_2(\text{H}_2\text{L})]^{2+}$  is 0.4 or lower. The high stability of the  $\text{O}\cdots\text{H}\cdots\text{O}$  hydrogen-bond fragment is therefore confirmed by the fact that it requires pH values of about 0.4 or less to protonate it, and it cannot be deprotonated at pH values up to 13.6.

Although protonation of  $\text{HL}^-$  to give  $\text{H}_2\text{L}$  might be expected to result in a blue shift of the m.l.c.t. transitions of the

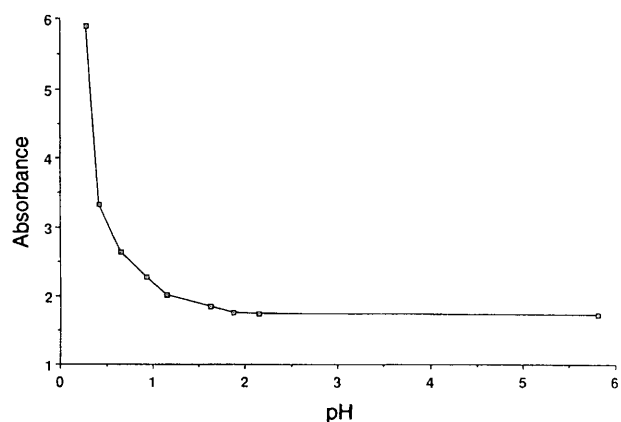


Fig. 6 Variation in intensity of the 298 nm transition of complex **1** with pH, in water: sample concentration,  $1.3 \times 10^{-5}\text{ mol dm}^{-3}$

complex<sup>14</sup> (from the arguments given earlier) in the range pH 2–0.4, we observed no significant variation in this region of the spectrum. This could be because the several overlapping m.l.c.t. transitions are poorly resolved and small changes in the positions of some shoulders would not be evident, but it is also consistent with our observation that the extent of intramolecular charge transfer in  $\text{HL}^-$  was not as large to start with as in other similar ligands.

### Electrochemistry of complex **1b**

Electrochemical measurements on complex **1b** show an intense, totally irreversible oxidation at +0.64 V *vs.* the ferrocene-ferrocenium couple which must be centred on  $\text{HL}^-$  since  $[\text{Ru}(\text{bipy})_3]^{2+}$  shows no such process. No such oxidation occurs for **2** (see later) at this potential, so the process must be unique to the monoprotonated  $\text{HL}^-$  form of the ligand rather than the fully deprotonated  $\text{L}^{2-}$  form. The expected  $\text{Ru}^{\text{II}}\text{--Ru}^{\text{III}}$  couple of **1b** is obscured by this process in the cyclic voltammogram, but the square-wave voltammogram shows a poorly resolved peak at *ca.* +1.0 V the potential of which is consistent with a  $[\text{Ru}(\text{bipy})_3]^{2+}$ -type group.<sup>13</sup> In contrast if  $\text{HL}^-$  were co-ordinated asymmetrically as an N,O-chelate the  $\text{Ru}^{\text{II}}\text{--Ru}^{\text{III}}$  couple would be at a much lower potential; that of  $[\text{Ru}(\text{bipy})_2(\text{hppy})]^+$  is at +0.03 V.<sup>2</sup> Three ligand-based reductions also occur, at -1.83, -2.05 and -2.62 V. The first two are fully reversible (peak-peak separation = 70–80 mV; cathodic and anodic peak currents equal) and at potentials characteristic of bipy-based reductions. The extreme negative potential of the third reduction means that it merges with the rise in current at the end of the solvent window, so its reversibility is difficult to assess even though its peak potential could be obtained from the square-wave voltammogram. This third reduction we assign to reduction of the co-ordinated  $\text{HL}^-$  since none of the reductions of  $[\text{Ru}(\text{bipy})_3]^{2+}$  occurs at such extreme potentials.<sup>13</sup>

### Electronic spectroscopy and electrochemistry of complex **2**

The oxidative cyclic and square-wave voltammograms of complex **2** in MeCN are in Fig. 7. There are two reversible, one-electron oxidations at +0.12 and +0.28 V which we assign to successive metal-centred  $\text{Ru}^{\text{II}}\text{--Ru}^{\text{III}}$  couples. The separation of 0.16 V between them gives a comproportionation constant  $K_c$  of *ca.* 650, which is a value characteristic of moderately coupled class II mixed-valence states. For the mixed-valence state a valence-localised (2,3) description of the oxidation states is therefore more appropriate than the  $(2\frac{1}{2}, 2\frac{1}{2})$  description which applies to class III complexes having much higher values of  $K_c$ . The complex  $[\text{Ru}(\text{bipy})_2(\text{hppy})]^+$ , which is a mononuclear model for the two sites of **2**,<sup>2</sup> has its  $\text{Ru}^{\text{II}}\text{--Ru}^{\text{III}}$  couple at +0.03 V; the somewhat higher potential for the first oxidation of **2**

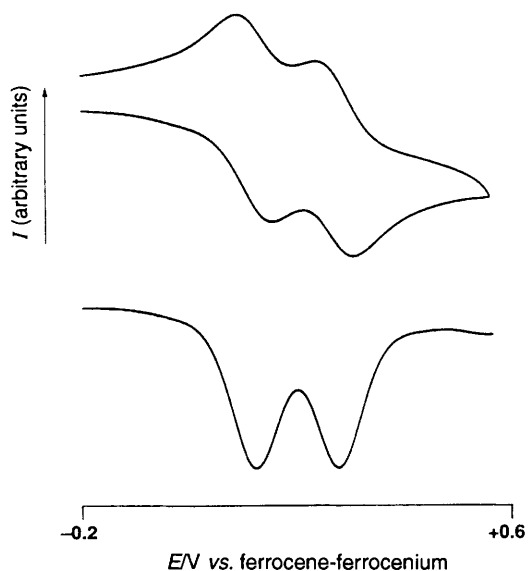


Fig. 7 Oxidative cyclic and square-wave voltammograms of complex 2 in MeCN

may be ascribed to the higher charge on the complex (+2 instead of +1). If the bridging ligand were co-ordinated in an asymmetric mode, resulting in  $\text{RuN}_6$  and  $\text{RuN}_4\text{O}_2$  centres, the two metal-based redox potentials would occur at much more widely separated potentials (related mononuclear complexes have redox potentials at *ca.* +0.9 and -0.5 V).<sup>13,15</sup>

Complex 2 also displays the expected four reductions at potentials characteristic of the terminal bipy ligands. These occur in closely overlapping pairs which result in two broad waves in the cyclic voltammogram centred at -1.93 and -2.22 V; the chemical reversibility of the processes on the electrochemical time-scale is indicated by the equal intensities of the cathodic and anodic waves. Square-wave voltammetry failed to resolve the first pair of reductions, which give a single peak at -1.93 V with intensity double that of the one-electron processes, but the second pair of bipy-based reductions is just resolved, with peaks at -2.20 and -2.26 V in the square-wave voltammogram.

The electronic spectra of complex 2 in the (2,2), (2,3) and (3,3) states are in Fig. 8. The mixed-valence complex was prepared by addition of exactly 0.5 equivalent of the two-electron oxidant  $[\text{NBu}_4][\text{Br}_3]$  to a solution of 2; the (3,3) state was prepared by addition of 1.2 equivalents of  $[\text{NBu}_4][\text{Br}_3]$  to ensure complete oxidation. The spectrum of the (2,2) complex displays an m.l.c.t. transition at 496 nm ( $\epsilon = 1.4 \times 10^4 \text{ dm}^3 \text{ mol}^{-1} \text{ cm}^{-1}$ ), with a low-energy shoulder at *ca.* 600 nm. There is also a transition at 366 nm ( $\epsilon = 2.0 \times 10^4 \text{ dm}^3 \text{ mol}^{-1} \text{ cm}^{-1}$ ) intensity of which suggests that it may be a higher-energy m.l.c.t. process. The intense peaks at 294 and 246 nm ( $\epsilon = 4.6$  and  $7.7 \times 10^4 \text{ dm}^3 \text{ mol}^{-1} \text{ cm}^{-1}$ , respectively) are the usual ligand-based  $\pi\text{-}\pi^*$  transitions.

Oxidation from the (2,2) to the (2,3) state has surprisingly little effect on the spectrum, which was examined out to 2000 nm. The lowest-energy m.l.c.t. transition moves from 496 to 490 nm; the higher-energy transitions are virtually unchanged in both position and intensity. The most significant feature is the emergence of a new, weak transition at 830 nm ( $\epsilon = 800 \text{ dm}^3 \text{ mol}^{-1} \text{ cm}^{-1}$ ) which looks like a good candidate for an intervalence charge-transfer (i.v.c.t.) band. However, on further oxidation to the (3,3) state this peak does not disappear, which suggests that it is associated with the ruthenium(III) centre. To check this we recorded the spectrum of the oxidised mononuclear model complex  $[\text{Ru}^{\text{III}}(\text{bipy})_2(\text{hppy})]^{2+}$ , prepared by treating the ruthenium(II) complex with an excess of  $[\text{NBu}_4][\text{Br}_3]$  in MeCN; this complex shows a very similar weak transition at 820 nm ( $\epsilon = 200 \text{ dm}^3 \text{ mol}^{-1} \text{ cm}^{-1}$ ). By analogy

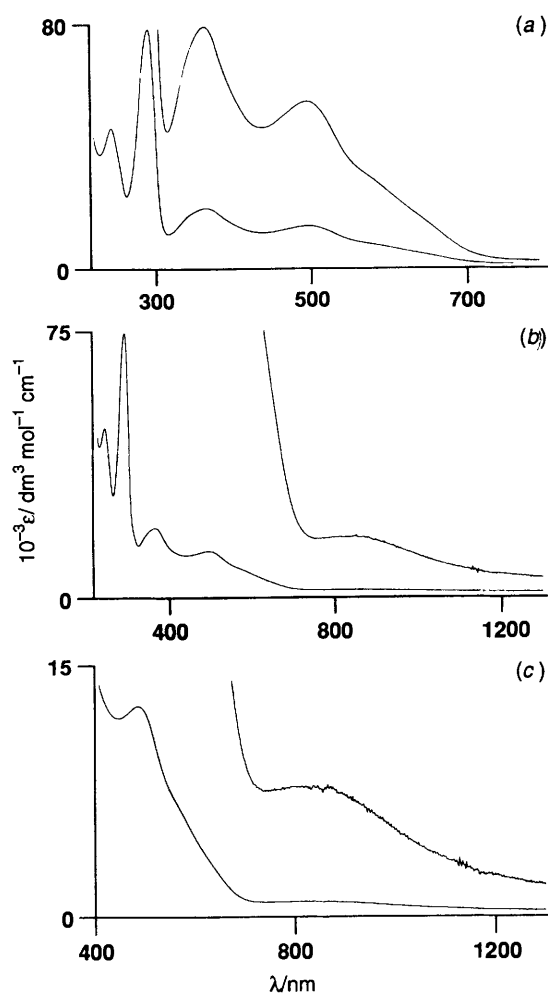


Fig. 8 Electronic spectra of complex 2 in the (a) (2,2), (b) (2,3) and (c) (3,3) oxidation states, all in MeCN. Expansions are  $\times 4$  (a),  $\times 20$  (b) and  $\times 10$  (c)

with the weak transition of  $[\text{Ru}(\text{bipy})_3]^{3+}$  which occurs at 680 nm ( $\epsilon = 400 \text{ dm}^3 \text{ mol}^{-1} \text{ cm}^{-1}$ ),<sup>16</sup> this is a pyridyl-to- $\text{Ru}^{\text{III}}$  (ligand-to-metal charge transfer l.m.c.t.) band. There is therefore no identifiable i.v.c.t. transition in the mixed-valence state. Such a band would certainly be expected, but given the modest  $K_c$ , value it may be at relatively high energy (in the 800–1000 nm range) and rather weak (dinuclear ruthenium complexes with comparable values of  $K_c$  can have  $\epsilon < 100 \text{ dm}^3 \text{ mol}^{-1} \text{ cm}^{-1}$ )<sup>1</sup> in which case it would be obscured by the l.m.c.t. band. The fact that a transition characteristic of a localised ruthenium(III) centre appears in the spectrum of the mixed-valence complex confirms that the mixed-valence state is a localised (2,3) species.

#### Attempts to prepare dinuclear complexes with $\text{L}^{2-}$ acting as an asymmetric bridge

Complex 1 could be an appealing building-block for polynuclear complexes by co-ordination of additional metal fragments at the peripheral O,O'-chelating site. We tried initially with second-row transition-metal fragments; however this was unsuccessful. For example, reaction of 1 with  $[\text{Ru}(\text{bipy})_2(\text{H}_2\text{O})_2]^{2+}$  at temperatures up to 190 °C afforded only unreacted 1 in addition to various by-products such as  $[\text{Ru}(\text{bipy})_3]^{2+}$ . Addition of base (KOH,  $\text{KOBU}$ ) to remove the proton protecting the O,O' site made no difference. Reaction of 1 with  $[\text{Pd}(\text{bipy})\text{Cl}_2]$  in basic ethanol was similarly unsuccessful even though  $[\text{Pd}(\text{bipy})\text{Cl}_2]$  reacts smoothly with catechol ( $\text{H}_2\text{cat}$ ) to give  $[\text{Pd}(\text{bipy})(\text{cat})]$  under the same conditions.<sup>17</sup> Molecular modelling studies showed that for the two oxygen

atoms of **1** to chelate to another second-row metal ion would require them to be *ca.* 2.8 Å apart, which would be difficult to attain given that the flexibility of the ligand is limited by the coordination of the N,N'-donor site.

Small, oxophilic first-row metal ions have more promise. Addition of iron(III) salts to aqueous solutions of complex **1** (as the nitrate salt) results immediately in a change to deep brown, and addition of NH<sub>4</sub>PF<sub>6</sub> results in a brown precipitate which is not unreacted **1**. This complex, and others based on coordination of first-row ions to the peripheral O,O' site of **1**, are currently being investigated.

## Conclusion

The compound H<sub>2</sub>L can co-ordinate to Ru<sup>II</sup> in two ways. It can act as a mononucleating ligand *via* the N,N'-donor binding site, which has the twin advantages of forming a planar, five-membered chelate ring and an intramolecular O...H...O hydrogen bond between the peripheral oxygen atoms. Alternatively it can form a dinuclear complex *via* a 'symmetric' co-ordination mode with two N,O-donor binding pockets, and two six-membered chelate rings. The 'asymmetric' dinucleating mode is sterically difficult for second-row metals since N,N'-chelation requires the ligand to be planar whereas O,O'-chelation requires it to be substantially twisted.

## Acknowledgements

We thank the EPSRC for financial support, and one of the referees for some helpful comments.

## References

- 1 M. D. Ward, *Chem. Soc. Rev.*, 1995, **24**, 121 and refs. therein.
- 2 B. M. Holligan, J. C. Jeffery, M. K. Norgett, E. Schatz and M. D. Ward, *J. Chem. Soc., Dalton Trans.*, 1992, 3345.
- 3 B. P. Sullivan, D. J. Salmon and T. J. Meyer, *Inorg. Chem.*, 1978, **17**, 3334.
- 4 M. Tiecco, M. Tingoli, L. Testaferri, D. Chianelli and E. Wenkert, *Tetrahedron*, 1986, **42**, 1475.
- 5 M. Tiecco, L. Testaferri, M. Tingoli, D. Chianelli and M. Montanucci, *Synthesis*, 1984, 736.
- 6 M. Iyoda, H. Otsuka, K. Sato, N. Nisato and M. Oda, *Bull. Chem. Soc. Jpn.*, 1990, **63**, 80.
- 7 C. Dietrich-Buchecker and J.-P. Sauvage, *Tetrahedron*, 1990, **46**, 503.
- 8 K. Nakamura, *Bull. Chem. Soc. Jpn.*, 1982, **55**, 2697; J. Rebek, jun., T. Costello and R. Wattley, *J. Am. Chem. Soc.*, 1985, **107**, 7487.
- 9 A. Chakravorty, *Coord. Chem. Rev.*, 1974, **13**, 1.
- 10 A. Novak, *Struct. Bonding (Berlin)*, 1974, **18**, 177.
- 11 B. M. Holligan, J. C. Jeffery and M. D. Ward, *J. Chem. Soc., Dalton Trans.*, 1992, 3337; J. C. Jeffery, E. Schatz and M. D. Ward, *J. Chem. Soc., Dalton Trans.*, 1992, 1921.
- 12 G. V. Long, S. E. Boyd, M. M. Harding, I. E. Buys and T. W. Hambley, *J. Chem. Soc., Dalton Trans.*, 1993, 3175.
- 13 A. Juris, V. Balzani, F. Barigeletti, S. Campagna, P. Belser and A. von Zelewsky, *Coord. Chem. Rev.*, 1988, **84**, 85.
- 14 P. J. Giordano, C. R. Bock and M. S. Wrighton, *J. Am. Chem. Soc.*, 1978, **100**, 6960; M. Haga, *Inorg. Chim. Acta*, 1983, **75**, 29.
- 15 D. A. Bardwell, D. Black, J. C. Jeffery, E. Schatz and M. D. Ward, *J. Chem. Soc., Dalton Trans.*, 1993, 2321.
- 16 G. M. Bryant and J. E. Ferguson, *Aust. J. Chem.*, 1971, **24**, 275.
- 17 K. H. Puthraya and T. S. Srivastava, *Polyhedron*, 1985, **4**, 1579.

*Received 2nd October 1995; Paper 5/06471F*